# Sensitive spectrophotometric determination of hydrogen peroxide in aqueous samples from advanced oxidation processes: Evaluation of possible interferences

**A. Rubio-Clemente[a],[b]*, A. Cardona[b], E. Chica[c] and G.A. Peñuela[b]**

[a]Facultad de Ciencias de la Salud, Universidad Católica San Antonio UCAM, Avenida de los Jerónimos, 135, C.P. 30107, Guadalupe-Murcia, España. [b]Grupo GDCON, Facultad de Ingeniería, Sede de Investigaciones Universitarias (SIU), Universidad de Antioquia UdeA, A.A. 1226, Calle 70, No. 52-21, Medellín, Colombia. [c]Departamento de Ingeniería Mecánica, Facultad de Ingeniería, Universidad de Antioquia UdeA, A.A. 1226, Calle 70, No. 52-21, Medellín, Colombia.

*Determinación espectrofotométrica sensible del peróxido de hidrógeno en muestras de agua procedentes de procesos de oxidación avanzada: Evaluación de posibles interferencias*

*Determinació espectrofotomètrica sensible del peròxid d'hidrogen en mostres d'aigua procedents de processos d'oxidació avançada: Avaluació de possibles interferències*

RECEIVED: 11 NOVEMBER 2016; REVISED: 6 DECEMBER 2016; ACCEPTED: 9 JANUARY 2017

## SUMMARY

Hydrogen peroxide ($H_2O_2$) determination in real water samples was carried out in a simple and sensitive way. The resulting optimal operating conditions from a $2^3$ full factorial experimental design were 450 nm, 50 mm and $6x10^{-3}$ M for the absorption wavelength, the quartz cell path length and the final concentration of the ammonium monovanadate solution, respectively; allowing the quantification of $H_2O_2$ up to $2.94x10^{-3}$ mM. The proposed analytical method was validated and the effect of the background matrix was investigated, obtaining a selective method. Additionally, the developed analytical method was applied for studying the evolution of $H_2O_2$ in the decontamination of water containing $6.73x10^{-5}$ mM of anthracene and $1.19x10^{-5}$ mM of benzo[a]pyrene using the UV/$H_2O_2$ system. It was found that the optimal $H_2O_2$ level enabling about 45% of mineralisation and a removal of the target polycyclic aromatic hydrocarbons higher than 99% was $2.94x10^{-1}$ mM, remaining approximately $1.47x10^{-1}$ mM of $H_2O_2$ after 90 min of treatment.

**Keywords:** Advanced oxidation process; ammonium monovanadate; matrix background; residual hydrogen peroxide; spectrophotometry

## RESUMEN

La determinación de peróxido de hidrógeno ($H_2O_2$) en muestras de agua real se llevó a cabo de una manera sencilla y sensible. Las condiciones óptimas de funcionamiento resultantes de un diseño experimental factorial completo fueron 450 nm, 50 mm y 6 x $10^{-3}$ M de longitud de onda de absorción, longitud de trayectoria de la celda de cuarzo y concentración final de la solución de monovanadato de amonio, respectivamente; permitiendo la cuantificación de $2.94x10^{-3}$ mM de $H_2O_2$. Se validó el método analítico propuesto y se investigó el efecto de la matriz obteniendo un método selectivo. Además, se aplicó el método analítico desarrollado para estudiar la evolución de $H_2O_2$ en la descontaminación de agua que contenía $6,73x10^{-5}$ mM de antraceno y $1,19x10^{-5}$ mM de benzo[a]pireno utilizando el sistema UV/$H_2O_2$. Se encontró que el nivel óptimo de $H_2O_2$ que permitía cerca del 45% de mineralización y una eliminación de los hidrocarburos aromáticos policíclicos objeto de estudio superior al 99% fue de $2,94x10^{-1}$ mM, perma-

***Corresponding author: ainhoa.rubioc@udea.edu.co**

neciendo aproximadamente 1,47x10$^{-1}$ mM de $H_2O_2$ después de 90 min de tratamiento.

**Palabras clave:** Proceso de oxidación avanzada; monovanadato de amonio; constituyentes de la matriz; peróxido de hidrógeno residual; espectrofotometría.

## RESUM

La determinació de peròxid de hidrogen ($H_2O_2$) en mostres autentiques d'aigua va ser realitzada de forma simple i senzilla. Les condicions de treball optimes resultants d'un disseny experimental factorial complert $2^3$ van ser de 450 nm, 50 mm i 6x10$^{-3}$ M per la longitud de onda d'absorció, la longitud de la trajectòria de les cubetes de quars i la concentració final de la solución de monovanadato de amoni, respectivament; això va permetre una quantificació de 2,94x10$^{-3}$ mM de $H_2O_2$. Es va avaluar el mètode d'anàlisi proposat i es va investigar l'efecte de la matriu de fons, obtenint un mètode selectiu. Addicionalment, el mètode analític desenvolupat es va aplicar per estudiar la evolució del $H_2O_2$ en la descontaminació del aigua que contenia 6,73x10$^{-5}$ mM de antracens i 1,19x10$^{-5}$ mM de benzo(a)pireno, fent servir el sistema UV/$H_2O_2$. Es va descobrir que el nivell òptim de $H_2O_2$ capaç de una mineralització del 45% i de una eliminació dels hidrocarburs aromàtics policíclics major del 99% era de 2,94x10$^{-1}$ mM, quan era aproximadament de 1,47x10-1 mM de $H_2O_2$ després de 90 minuts de tractament.

**Paraules clau:** Procés de oxidació avançat; monovanadato de amoni; matriu de fons; peròxid de hidrogen residual; espectrofotometria

## INTRODUCTION

Hydrogen peroxide ($H_2O_2$) is a manufactured product but it can be naturally found at low concentrations in atmospheric, soil and aqueous ecosystems[1,2]. $H_2O_2$ is widely used for water treatment purposes. With an oxidation potential of 1.763 V[3], $H_2O_2$ is known to be a powerful oxidant[4], able to oxidise organic pollutants. However, the greater relevance of using $H_2O_2$ for water treatment mainly resides in its ability to undergo photolysis in contact with UV radiation, producing hydroxyl radicals (HO°)[5], whose standard electrode potential is higher than that of $H_2O_2$ (E°=2.80 V)[6] and, subsequently, is able to remove a larger amount of organic pollutants[7].

The photolytic ability of $H_2O_2$ is exploited by several advanced oxidation processes (AOPs), such as UV/$H_2O_2$, UV/$O_3$/$H_2O_2$, UV/US/$H_2O_2$ and photo-Fenton (UV/$Fe^{2+,3+}$/$H_2O_2$) systems, among other processes.

Recently, a great number of works reporting the efficiency of AOPs for degrading persistent and recalcitrant toxics has been published[7-10]. Due to the demonstrated effectiveness of using $H_2O_2$ in both photolytic and non-photolytic AOPs, its determination is of special interest for efficient water decontamination. Additionally, considering that an excess of $H_2O_2$ is involved in HO° scavenging processes, and because of it is a costly reagent[11], the analysis of $H_2O_2$ is even more significant when it is added in a continuous way in order to know when a new addition of $H_2O_2$ is required for the oxidation of pollutants to continue.

On the other hand, there are other AOPs where $H_2O_2$ is generated. This is the case of heterogeneous photo-catalysis processes using semiconductors such as $TiO_2$. When $TiO_2$ is illuminated and a photon with energy above its bandgap energy is absorbed, a pair hole ($h^+$)–electron ($e^-$) is formed. Both the $h^+$ and $e^-$ can oxidise and reduce $H_2O$ and $O_2$, respectively, resulting in the production of $H_2O_2$. The generated $H_2O_2$ acts to prevent the recombination of $h^+$ and $e^-$[7], leading to a higher decontamination. However, although the generation of $H_2O_2$ has a positive effect, residual $H_2O_2$ can also pose a risk for the living beings in the receptor systems of the AOP effluent. $H_2O_2$ is a widely recognised biocide, since it may interact with organism biomolecules, causing their oxidation[12]. Therefore, the quantification of $H_2O_2$ is essential for both water treatment and ecosystem conservation purposes.

Several techniques for $H_2O_2$ determination in solid, gas and aqueous samples have been reported[2,13-16]. For $H_2O_2$ analysis in water, one of the most applied methods is the permanganate titration. However, it is interfered by $Fe^{2+}$ ions, which are catalysing agents in Fenton and photo-Fenton systems, due to the complexes formed between theses ions and permanganate[14]. In turn, the use of enzyme-catalysed reactions can be a quite sensitivity method; nevertheless, the use of enzyme requires strict experimental conditions, limiting the application of this technology. Under this scenario, Pupo Nogueira and co-workers[14] proposed a colorimetric method based on the formation of complexes between $H_2O_2$ and ammonium monovanadate in acidic medium. Even though this method can be applied for a wide range of water samples, it does not allow analysing $H_2O_2$ at residual levels, since its limit of quantification is 2.5x10$^{-2}$ mM[14]. In this sense, the current work aims at extending this limit of quantification. Additionally, the interfering substances commonly found in water matrices, such as $Fe^{3+}$, $Fe^{2+}$, $Cl^-$, $NO_3^-$, $PO_4^{3-}$, $NH_4^+$, $Mg^{2+}$, $Na^+$, $Mn^{2+}$, $F^-$, $K^+$, $CO_3^{2-}$ and $Ca^{2+}$, were evaluated. Furthermore, the proposed analytical method was validated and applied to study the $H_2O_2$ evolution in real natural water treated using the UV/$H_2O_2$ system.

## MATERIALS AND METHODS

### Reagents and chemicals

All reagents were analytical grade and the solutions were prepared in deionised water. The used reagents were hydrogen peroxide, 30% w/w ($H_2O_2$, J.T. Baker); acetonitrile, gradient grade (Merck); orthophosphoric acid, 85% ($H_3PO_4$, Carlo Erba); fuming hydrochloric acid, 37% (HCl, Merck); ammonium hydroxide, 28-30% ($NH_4OH$, Mallinckrodt); nitric acid, 65% ($HNO_3$,

Merck); ammonium monovanadate, 99.9% ($NH_4VO_3$, Merck); sulfuric acid, 95-97% ($H_2SO_4$, Merck); calcium carbonate ($CaCO_3$, Carlo Erba); sodium carbonate ($Na_2CO_3$, Merck); ammonium sulfate ($(NH_4)_2SO_4$, Mallinckrodt); iron (II) sulfate heptahydrate ($Fe_2SO_4$ $7H_2O$, Sigma-Aldrich); iron (III) chloride hexahydrate ($FeCl_3$ $6H_2O$, Panreac); standard solution of iron (III) nitrate ($Fe(NO_3)_3$, Merck); manganese (II) sulfate monohydrate ($MnSO_4$ $H_2O$, Merck); anthracene 99% and benzo[a]pyrene 96% (Alfa Aesar).

### Solutions

Standard stock solutions of $H_2O_2$ were prepared by diluting suitable amounts of $H_2O_2$. $H_2O_2$ working solutions were prepared by diluting the stock solutions of $H_2O_2$ and a calibration curve was built from $2.94x10^{-3}$ to $4.41x10^{-1}$ mM. Additionally, a 0.06 M $NH_4VO_3$ stock solution was prepared by using a 0.36 M $H_2SO_4$ stock solution and completing with deionised water.

### $H_2O_2$ analysis procedure and apparatus

The optimal procedure for the determination of $H_2O_2$ in water samples consisted of adding 40 mL of the sample to be analysed and 5 mL of the $NH_4VO_3$ stock solution in a 50 mL flask. Deionised water was added to the mark and the mixture was transferred to the quartz cell. The control standards of this procedure corresponding to the low, medium and high levels of the calibration curve were $2.94x10^{-3}$, $5.88x10^{-2}$ and $4.41x10^{-1}$ mM, respectively. In addition, a reagent blank was performed by adding 5 mL of the $NH_4VO_3$ stock solution into a 50 mL volumetric flask and diluting with deionised water to the mark. With this reagent blank, the baseline of the spectrophotometer was built.

Spectrophotometric studies were carried out using a UV–Vis spectrophotometer Evolution 300 (Thermo Scientific) and a quartz cell of 50 mm optical path length (Macherey-Nagel), unless indicated otherwise. Measures of absorbance were taken by triplicate using a Xenon lamp at a wavelength of 450 nm, unless specified otherwise. For the analysis of anthracene and benzo[a]pyrene, an Agilent RP-HPLC system (series 1100/1200) with a fluorescence detector was used under the operating conditions specified elsewhere[17]. Total organic carbon was measured using an Apollo 9000 series total organic carbon analyser (Teledyne Tekmar).

### Experimental design and irradiation tests

In order to determine the most favourable conditions for $H_2O_2$ quantification, a $2^3$ full factorial experimental design was used. The influence of the final concentration of $NH_4VO_3$ reacting with $H_2O_2$ in the sample, the absorption wavelength and the quartz cell path length were studied at two main levels. This experimental design resulted in 8 runs, executed in a randomised order. The considered responses were the absorbance maximisation of the calibration curve levels at $2.94x10^{-3}$; $5.88x10^{-2}$ and $4.41x10^{-1}$ mM; and the maximisation of the correlation coefficient ($R^2$). Statgraphics Centurion XVII program package (StatPoint Technologies) was used for the statistical analysis of the data with a confidence interval of 95%.

UV/$H_2O_2$ photo-degradation experiments were carried out in batch mode using a 2 L annular borosilicate glass photo-reactor. One and three 8 W Hg low-pressure lamps emitting at 254 nm and contained in different quartz tubes were used. The irradiation intensity was measured with a UVX radiometer equipped with a UVX-25 sensor (UVP), resulting to be of 170 and 460 μW/cm$^2$ for 1 and 3 UV-C lamps, respectively. The photo-reactor was equipped with a cooling jacket, allowing maintaining constant the bulk temperature. The irradiated solution was natural water from "El Peñol" dam, located in Guatapé (Antioquia, Colombia), which was spiked with $6.73x10^{-5}$ and $1.19x10^{-5}$ mM of anthracene and benzo[a]pyrene, respectively.

## RESULTS AND DISCUSSION

### Preliminary assumptions

As it is widely known, the absorbance of a substance can be expressed as Equation (1).

$$A = \varepsilon bc \qquad (1)$$

where A is the absorbance of the chemical species; ε, the molar absorptivity coefficient or molar attenuation coefficient, related to the absorption wavelength; b, the optical path length of the cell containing the sample; and c, the concentration of the target substance.

According to Pupo Nogueira and co-workers[14], $H_2O_2$ reacts with ammonium monovanadate in acidic medium, yielding a peroxovanadium cation, characterised by its orangey-red colour, as indicated in Equation (2).

$$VO_3^- + 4H^+ + H_2O_2 \rightarrow VO_2^{3+} + 3H_2O \qquad (2)$$

Since the generated compound is able to absorb light, in order to determine the optimal wavelength at which the maximum absorption is obtained, a wavelength scan was performed in the range from 370 to 770 nm (Figure 1). As shown in the figure, a maximal absorption is located around 450 nm. Although this value was already reported[14], high absorptions were also evidenced at 454 nm. Therefore, for discerning which wavelength is the optimal one, both of the wavelength values were considered in the $2^3$ experimental design.

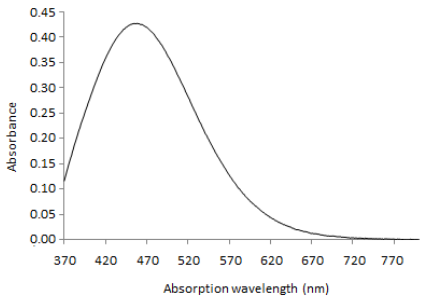


*Figure 1. UV-visible absorption spectrum of the peroxovanadium cation. $H_2O_2$ and $NH_4VO_3$ concentrations were $2.94x10^{-1}$ mM and $6x10^{-3}$ M, respectively.*

As indicated, the path length of the cell is a crucial factor in the spectrophotometric response regarding the amount of absorbed radiation, since a higher cell path length results in a higher amount of energy absorbed by the molecules in the sample. Therefore, lower quantification limits can be obtained with higher cell path lengths, allowing the determination of residual levels of $H_2O_2$. In this sense, two quartz cells of 10 and 50 mm path lengths were studied.

In addition to the absorption wavelength and the cell path length, previous experiments evidenced that the concentration of $NH_4VO_3$ in acidic medium influenced also the system[14]. The effect of the $NH_4VO_3$ level was ascribed to the number of the formed coloured peroxovanadium cation, which were dependent on the amount of $H_2O_2$ and the final reacting level of $NH_4VO_3$. In order to determine the optimal concentration of $NH_4VO_3$ for forming coloured peroxovanadium cations, $6x10^{-3}$ and $1.2x10^{-2}$ M final solution levels in the 50 mL flask were tested. In turn, unlike $NH_4VO_3$, $H_2SO_4$ was not observed to influence the system[14]. Therefore, its effect was not studied and a final solution of 0.036 M $H_2SO_4$ was used during the optimization step and analysis of $H_2O_2$. This concentration of $H_2SO_4$ provided the reaction medium with the required acidic conditions (pH < 2) for the generation of peroxovanadium cations, avoiding using high concentrations of acid.

## Optimal condition experiments

The absorption wavelength, the cell path length and the final concentration of $NH_4VO_3$ were considered as factors affecting the spectrophotometric system. In order to find the optimal set of values for those factors, a full factorial experimental design was used in water samples spiked with a concentration of $2.94x10^{-1}$ mM $H_2O_2$. The studied levels of $NH_4VO_3$ final concentration, absorption wavelength and quartz cell path length were $6x10^{-3}$–$1.2x10^{-2}$ M, 450-454 nm and 10-50 mm, respectively. The optimisation goal was to maximise the absorption for the low, medium and high level, corresponding to $2.94x10^{-3}$, $5.88x10^{-2}$ and $4.41x10^{-1}$ mM $H_2O_2$, as well as to obtain an excellent $R^2$.

Analysis-of-variance tests were used to find the statistically significant factors for the considered domain. Graphically, the significance of the examined parameters can be observed from the Pareto plots of the considered responses (Figure 2). This graphical tool informs about the estimated effect of each factor through bars, where the bar at the top corresponds to the most statistically significant factor. In turn, the vertical line refers to the value beyond which all the bars exceeding it are considered statistically significant under a significance level of 5%. Thus, as shown in Figure 2a, 2b and 2c, the quartz cell path length is the sole main factor significantly influencing the system for the responses related to the absorption at a low, medium and high level, with a confidence interval of 95%. It was found that the influence of the cell path length was positive. As expected, an increase in the irradiated path length resulted in a higher absorption at the three considered levels. For $R^2$ (Figure 2d), none of the examined parameters resulted to be statistically significant. A possible explanation can be found in the fact that the obtained responses were quite similar for all of the executed runs.

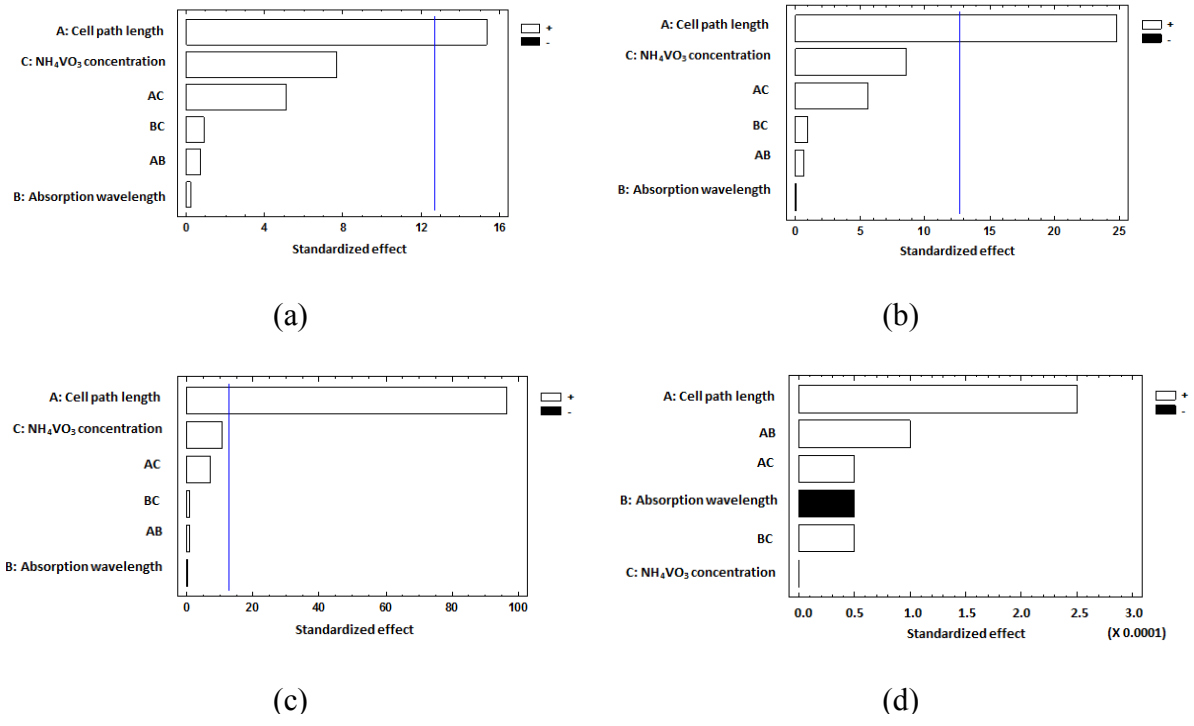


**Figure 2.** *Pareto charts for the absorbance at a low (a), medium (b) and high (c) level, and for the $R^2$ (d). The black and white colours indicate the positive and negative effects, respectively, of the considered factors and interactions. Working ranges: $6x10^{-3}$–$1.2x10^{-2}$ M ($NH_4VO_3$ final concentration), 450–454 nm (absorption wavelength) and 10–50 mm (cell path length). $[H_2O_2]_o$=$2.94x10^{-1}$ mM.*

Consequently, the quartz cell path length was considered at its high level; i.e., a cell path length of 50 mm was used for subsequent studies. With regard to the final concentration of $NH_4VO_3$ solution, due to it was statistically non-significant for the investigated conditions and in order to save in reagent costs, it was used at its low level (i.e., at $6x10^{-3}$ M).

As far as the absorption wavelength is concerned, even though it is a parameter of great importance in spectrometry, for this study it was statistically non-significant under a confidence interval of 95% because of the low range studied, from 450 to 454 nm. Nevertheless, from the $R^2$ results, higher values were achieved at 450 nm. Therefore, this absorption wavelength was selected as the optimal one.

The constructed models for the absorbance at the low (Abs LL), medium (Abs ML), and high (Abs HL) level, as well as for the $R^2$, with adjusted R-squared statistics higher than 97.5%, are expressed by Equations (3)-(6).

$$Abs\ LL = 3.23513 - 0.0324875PL - 0.00715625AW - 0.163862AmV + 0.000071875PL * AW + 0.00021125PL * AmV + 0.003625AW * AmV \quad (3)$$

$$\text{Abs ML} = 3.24775 - 0.023925\text{PL} - 0.0071875\text{AW} - 0.1694\text{AmV} + 0.00005625\text{PL} * \text{AW} + 0.00021\text{PL} * \text{AmV} + 0.000375\text{AW} * \text{AmV} \quad (4)$$

$$Abs\ HL = 2.542 - 0.0169\text{PL} - 0.005625\text{AW} - 0.12425\text{AmV} + 0.0000625\text{PL} * \text{AW} + 0.00021\text{PL} * \text{AmV} + 0.000275\text{AW} * \text{AmV} \quad (5)$$

$$R^2 = 1.03887 - 0.0005625\text{PL} - 0.0000875\text{AW} - 0.0011375\text{AmV} + 0.00000125\text{PL} * \text{AW} + 2.5\text{E}-7\text{PL} * \text{AmV} + 0.0000025\text{AW} * \text{AmV} \quad (6)$$

where PL, AW and AmV correspond to the cell path length, the absorption wavelength and the final concentration of $NH_4VO_3$, respectively.

It is important to note that the main effect plot in Figure 3 shows that there were no curvature effects in the considered domain for the studied parameters. That was the reason why the quadratic terms were not included in the constructed models.

Hence, from the statistical analysis, the optimal operating conditions were 50 mm, $6x10^{-3}$ M and 450 nm for the quartz cell path length, the final concentration of $NH_4VO_3$ solution and the absorption wavelength, respectively.

## Validation of the developed analytical method

In order to evaluate the practical application of the proposed analytical method, performance parameters such as linearity, limit of quantification, precision and accuracy were measured under the optimal analysis conditions. Results of the validation parameters are given in Table 1.

**Table 1.** *Data obtained from the validation of the proposed analytical method*

| | Working range (mM) (n=3) | Inter-day precision (n=10) (RSD, %) | | | Accuracy (n=10) (absolute value and RSD, %) | | | Recovery (n=10) (absolute value and RSD, %) | |
|---|---|---|---|---|---|---|---|---|---|
| $H_2O_2$ | $2.94x10^{-3}$ – $4.41x10^{-1}$ | LL | ML | HL | LL | ML | HL | 30 | 70 |
| | | 10.14 | 1.89 | 0.87 | 87.87 (10.14) | 100.12 (1.90) | 99.87 (0.86) | 103.47 (13.97) | 99.71 (9.79) |
| LL: Low level ($2.94x10^{-3}$ mM) | | ML: Medium level ($5.88x10^{-2}$ mM) | | | HL: High level ($4.41x10^{-1}$ mM) | | | | |

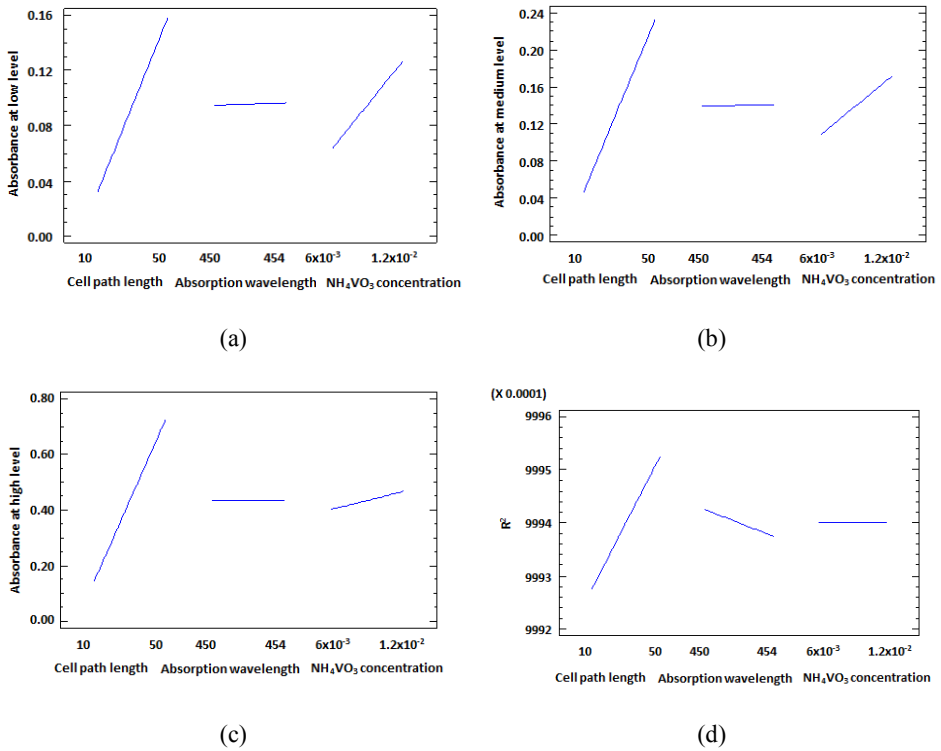


**Figure 3**. *Main effect plots for the absorbance at a low (a), medium (b) and high (c) level, and for the $R^2$ (d). Working ranges: $6x10^{-3}$–$1.2x10^{-2}$ M ($NH_4VO_3$ final concentration), 450–454 nm (absorption wavelength) and 10–50 mm (cell path length). $[H_2O_2]_o$=$2.94x10^{-1}$ mM.*

The linearity of the calibration curve was observed over a concentration range of $2.94x10^{-3}$–$4.41x10^{-1}$ mM for triplicate measurements and an excellent linearity, with a $R^2$ equal to 1, was achieved. The limit of quantification was found to be $2.94x10^{-3}$ mM. It is highlighted that concentration of $H_2O_2$ in water samples higher than $4.4x10^{-1}$ mM can be determined by appropriately diluting the sample of interest and introducing the correction factor when calculating the level of this species.

Additionally, the instrumental repeatability was also evaluated at $2.94x10^{-3}$ mM $H_2O_2$ and the relative standard deviation (RSD) resulted to be 0.96%, lower than the reference value of the spectrophotometer used in this study (1%). In turn, the inter-day precision and accuracy RSDs for the low, medium and high level were lower than 11%.

On the other hand, to analyse the applicability of the proposed analytical method, fresh natural water was used (n=10). Recoveries of the analyte were measured by speaking this matrix with $H_2O_2$ at concentrations levels of 30% and 70% (concentration factor) for $1.47x10^{-1}$ mM. As it can be observed from Table 1, quite acceptable recoveries were obtained.

## Matrix background. Evaluation of the interfering effect from ions

The effect of common ions present in water was investigated by measuring the absorbance of peroxovanadium complexes in acidic conditions. Several concentrations of foreign ions were studied using a standard solution of $2.94x10^{-1}$ mM $H_2O_2$ in deionised water under the determined optimal conditions. In Table 2 the levels of the studied ions and their tolerance limits, i.e., the highest concentration causing a signal variation lower than ± 5% in the absorbance, are listed. It was found that $Fe^{2+}$ was a major interfering substance, as well as $CO_3^{2-}$. The interfering effect of $Fe^{2+}$ at a concentration higher than 0.005 mM can be attributed to the Fenton reaction expressed by Equation (7). When $H_2O_2$ is in the bulk, it can react with $Fe^{2+}$, giving $HO^o$ and $Fe^{3+}$[18]. Therefore, the catalytic decomposition of $H_2O_2$ is produced and the higher the level of $Fe^{2+}$, the faster the reaction is produced; attaining an absorbance reduction. It is noteworthy that $Fe^{3+}$ can also react with $H_2O_2$ to regenerate $Fe^{2+}$, as indicated in Equation (8). However, the reaction rate constant ($k_2$) is 7600 times slower than $k_1$[10]. Therefore, for practical purposes, it can be affirmed that $Fe^{3+}$ does not influence the absorbance of the considered system.

$$Fe^{2+} + H_2O_2 \rightarrow Fe^{3+} + OH^- + HO^o; k_1 = 76\ M^{-1}s^{-1} \quad (7)$$

$$Fe^{3+} + H_2O_2 \rightarrow Fe^{2+} + H^+ + HO_2^o;\ k_2 = 0{,}01 - 0{,}02\ M^{-1}s^{-1} \quad (8)$$

With regard to $CO_3^{2-}$, changes in colour at the concentration of 25 mM using both $CaCO_3$ and $Na_2CO_3$ as $CO_3^{2-}$ sources were observed, resulting in an absorbance increase. Additionally, when $CaCO_3$ was used as the reactant for providing $CO_3^{2-}$, turbidity was also found at the level of 7.5 mM $CaCO_3$, being more noticeable for 50 mM $CaCO_3$. Nevertheless, by filtering the samples, suspended solids were removed.

**Table 2**. *Influence of coexisting ions for a solution of $2.94x10^{-1}$ mM of $H_2O_2$*

| Interference ion | Concentration range (mM) | Tolerance limit (mM) |
|---|---|---|
| $Fe^{3+}$ ($FeCl_3\ 6H_2O$), ($Fe(NO_3)_3$) | 0.001 - 1 | 1 |
| $Fe^{2+}$ ($FeSO_4\ 7H_2O$) | 0.001 - 1 | 0.005 |
| $Cl^-$ (HCl) | 0.05 - 1000 | 1000 |
| $NO_3^-$ ($HNO_3$) | 0.01 - 5 | 5 |
| $PO_4^{3-}$ ($H_3PO_4$) | 0.001 - 1 | 1 |
| $NH_4^+$ ($NH_4OH$) | 0.01 - 10 | 10 |
| $Mg^{2+}$ ($MgSO_4\ 7H_2O$) | 0.001 - 1 | 1 |
| $Na^+$ (NaCl) | 0.05 - 75 | 75 |
| $Mn^{2+}$ ($MnSO_4\ H_2O$) | 0.001 - 1 | 1 |
| $F^-$ (NaF) | 0.001 - 1 | 1 |
| $K^+$ (KCl) | 0.05 - 75 | 75 |
| $Ca^{2+}$ (CaCl) | 0.05 - 50 | 50 |
| $CO_3^{2-}$ ($CaCO_3$), ($Na_2CO_3$) | 0.01 - 50 | 15 |

From these results, it can be asserted that the proposed analytical method is quite selective for the determination of low levels of $H_2O_2$ in different kinds of water.

## Application to real samples. Photo-degradation experiments

The studied method was applied for the determination of residual $H_2O_2$ in natural water samples treated with the UV/$H_2O_2$ advanced oxidation system in the annular photo-reactor described above. Natural water was taken from "El Peñol" dam, located in Guatapé (Colombia), whose characteristics are summarised in Table 3.

**Table 3.** *"El Peñol" dam water characteristics*

| Parameter | Value |
|---|---|
| Temperature (°C) | 23.58 |
| pH | 7.35 |
| Dissolved oxygen ($mgO_2\ L^{-1}$) | 8.61 |
| Total organic carbon ($mgC\ L^{-1}$) | 2.03 |
| Conductivity ($mS\ m^{-1}$) | 39.87 |
| Turbidity (NTU) | 1.09 |
| Redox potential (meV) | 222.59 |
| Dissolved Fe ($mg\ L^{-1}$) | < 0.05 |
| Total alkalinity ($mg\ CaCO_3\ L^{-1}$) | 16.33 |
| Total hardness ($mg\ CaCO_3\ L^{-1}$) | 17.67 |
| $NO_3^-$ ($mg\ L^{-1}$) | 2.99 |
| $Cl^-$ ($mg\ L^{-1}$) | 3.393 |
| $SO_4^{2-}$ ($mg\ L^{-1}$) | 1.949 |
| $PO_4^{3-}$ ($mg\ L^{-1}$) | 0.026 |
| Anthracene | n.d.* |
| Benzo[a]pyrene | n.d.* |
| *Non-detected. | |

The water was spiked with $6.73x10^{-5}$ mM anthracene and $1.19x10^{-5}$ mM benzo[a]pyrene. Different levels of $H_2O_2$ ($1.47x10^{-1}$; $2.94x10^{-1}$; $4.41x10^{-1}$ and $5.88x10^{-1}$ mM) were tested during a reaction time of 90 min. Additionally, the efficiency of 1 and 3 lamps UV-C lamps, corresponding to 8 and 24 W, respectively, was examined for anthracene and benzo[a]pyrene degradation. Measurements of anthracene and benzo[a] pyrene reduction, total organic carbon removal and $H_2O_2$ evolution were taken in three replicates at different time intervals. The samples were collected in glass containers, stored in the dark at 4 °C and treated as soon as possible.

$$H_2O_2 + h\nu \rightarrow 2HO^o \quad (9)$$

$$H_2O_2 + HO^o \rightarrow HO_2^o + H_2O \quad (10)$$

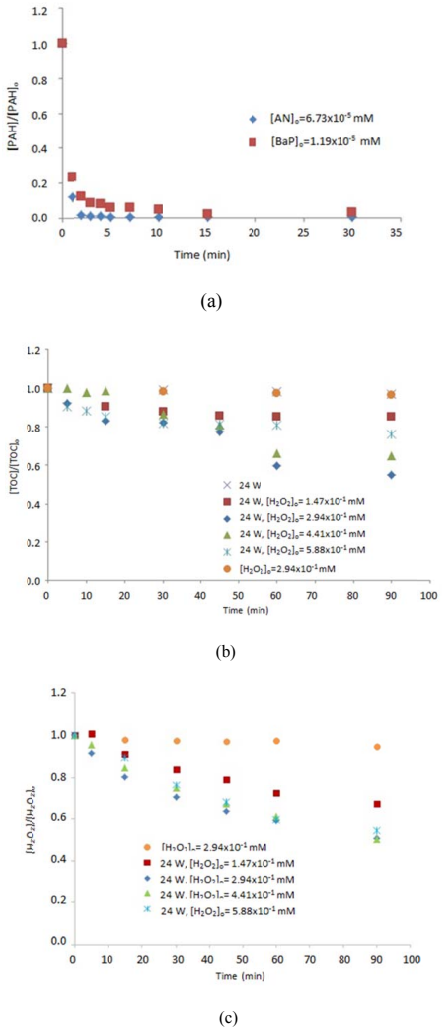


**Figure 4.** *(a) Anthracene (AN) and benzo[a]pyrene (BaP) removal using 1 UV-C lamp. (b) Total organic carbon (TOC) reduction. (c) $H_2O_2$ evolution. $[AN]_o$= 6.73x10$^{-5}$ mM; `[BaP] $_o$= 1.19x10$^{-5}$ mM; $[TOC]_o$=2.04 mgC L$^{-1}$; $[H_2O_2]_o$=1.47x10$^{-1}$, 2.94x10$^{-1}$, 4.41x10$^{-1}$ and 5.88x10$^{-1}$ mM; UV-C lamps=1 and 3 lamps, corresponding to 8 and 24 W, respectively.*

When $H_2O_2$ is irradiated, it interacts with photons, generating HO°, as expressed by Equation (9). The formed HO° reacts with the water organic matter, oxidising it and forming reaction intermediate products up to a complete mineralisation to form $H_2O$ and $CO_2$. As illustrated in Figure 4a, a removal of anthracene and benzo[a]pyrene higher than 99% was achieved in 30 min of irradiation with 1 UV-C lamp and without the use of $H_2O_2$. This is due to the absorbance properties of these compounds at 254 nm[19], especially of anthracene. However, this result did not assure the mineralisation of the target compounds. In fact, in Figure 4b, which represents the evolution of the total organic carbon, it can be observed that the mineralisation attained by using 3 UV-C lamps without $H_2O_2$ was < 5%. Although the obtained value of organic matter is within the range allowable in the legislation for drinking water, the mineralisation of the target compounds is not assured, and the presence of degradation by-products with a toxicity even higher than that of the parent compounds can occur. Hence, the mineralisation evolution must be studied combining the action of 3 UV-C lamps and adding different amounts of $H_2O_2$. As illustrated in the figure, the use of 3 UV-C lamps and 2.94x10$^{-1}$ mM of $H_2O_2$ resulted in a sample mineralisation of about 45% after 90 min of reaction time. Additionally, under these working conditions, no toxic reaction intermediate products were evidenced. Therefore, these operating conditions allowed an efficient conversion of anthracene and benzo[a]pyrene to harmless degradation by-products. Moreover, the higher the organic matter removal, the lower the possibility of disinfection by-product formation.

With regard to the evolution of $H_2O_2$, Figure 4c shows that 2.94x10$^{-1}$ mM $H_2O_2$ remained almost constant throughout the reaction time when dark conditions were used, which was expected since in Figure 4b the total organic carbon removal by using this level of $H_2O_2$ in the dark can be neglected. On the other hand, when $H_2O_2$ is irradiated, there is a $H_2O_2$ reduction during the reaction time because of the formation of HO°, as indicated in Equation (9). High reductions of $H_2O_2$ were observed when 2.94x10$^{-1}$; 4.41x10$^{-1}$ and 5.88x10$^{-1}$ mM were used. However, higher levels of total organic carbon removal were found when 2.94x10$^{-1}$ mM $H_2O_2$ was added to the reaction medium. This result indicated that levels of $H_2O_2$ higher than 2.94x10$^{-1}$ mM resulted in an unnecessary reagent cost, since an excess of $H_2O_2$ can also act as a quencher of HO°, as expressed in Equation (10); subsequently, reducing the efficiency of the oxidation system.

## CONCLUSION

In the current work, an analytical method for the determination of the residual and/or produced $H_2O_2$ from AOPs for water decontamination was developed in a simple and rapid way. The effects of the quartz cell path length, the final concentration of the $NH_4VO_3$ solution and the absorption wavelength were studied. The optimal conditions allowing the quantification of $H_2O_2$ in natural water were 450 nm of absorption wavelength, 50 mm of quartz cell path length and 6x10$^{-3}$ M of $NH_4VO_3$ final concentration solution. The developed method was validated and the influence of several ions commonly present in water was examined, resulting to be a selective method. In this sense, due to the achieved low quantification limit and because of the proposed analytical method is relatively free from interferences; it can be used for several types of water. In fact, it was applied for studying the evolution of $H_2O_2$ in the decontamination of real natural water spiked with anthracene and benzo[a]pyrene at a level of 6.73x10$^{-5}$ and 1.19x10$^{-5}$ mM, respectively. It was found that after 90 min of treatment and using 3 UV-C lamps, approximately 1.47x10$^{-1}$ mM $H_2O_2$ were consumed obtaining a reduction of the total organic carbon around 45% and a removal of anthracene and benzo[a]pyrene higher than 99%.

## ACKNOWLEDGEMENTS

This work was supported by the Spanish Agency for International Development Cooperation (AECID), the Colombian Administrative Department of Science, Technology and Innovation (COLCIENCIAS), and the Sustainability Fund of Universidad de Antioquia.

## REFERENCES

1. Kormann, C.; Bahnemann, D. W.; Hoffmann, M. R. Photocatalytic production of $H_2O_2$ and organic peroxides in aqueous suspensions of $TiO_2$, ZnO, and desert sand. *Environ. Sci. Technol.* **1988,** *22*, 798-806.
2. Olasehinde, E. F.; Makino, S.; Kondo, H.; Takeda, K.; Sakugawa, H. Application of Fenton reaction for nanomolar determination of hydrogen peroxide in seawater. *Anal. Chim. Acta* **2008**, *627*, 270-276.
3. Bratsch, S. G. Standard electrode potentials and temperature coefficients in water at 298.15 K. *J. Phys. Chem. Ref. Data* **1989**, *18*, 1-21.
4. Chen, H.; Yu, H.; Zhou, Y.; Wang, L. Fluorescent quenching method for determination of trace hydrogen peroxide in rain water. *Spectrochim. Acta Part A* **2007,** *67*, 683-686.
5. Kralik, P.; Kusic, H.; Koprinavac, N.; Bozic, A. L. Degradation of chlorinated hydrocarbons by UV/$H_2O_2$: the application of experimental design and kinetic modeling approach. *Chem. Eng. J.* **2010**, *158*, 154-166.
6. Rubio-Clemente, A.; Chica, E.; Peñuela, G. A. Application of Fenton process for treating petrochemical wastewater. Ing. Compet. **2014**, *16*, 211-223.
7. Rubio-Clemente, A.; Torres-Palma, R. A.; Peñuela, G. A. Removal of polycyclic aromatic hydrocarbons in aqueous environment by chemical treatments: a review. *Sci. Total Environ.* **2014**, *478*, 201-225.
8. Karci, A. Degradation of chlorophenols and alkylphenol ethoxylates, two representative textile chemicals, in water by advanced oxidation processes: the state of the art on transformation products and toxicity. *Chemosphere* **2014**, *99*, 1-18.
9. Ribeiro, A. R.; Nunes, O. C.; Pereira, M. F. R.; Silva, A. M. T. An overview on the advanced oxidation processes applied for the treatment of water pollutants defined in the recently launched Directive 2013/39/EU. *Environ. Int.* **2015**, *75*, 33-51.
10. Rubio-Clemente, A.; Chica, E.; Peñuela, G. A. Petrochemical wastewater treatment by photo-Fenton process. *Water Air Soil Pollut.* **2015**, *226*, 61-79.
11. Comninellis, C.; Kapalka, A.; Malato, S.; Parsons, S. A.; Poulios, I.; Mantzavinos, D. Advanced oxidation processes for water treatment: advances and trends for R&D. *J. Chem. Technol. Biotechnol.* **2008**, *83*, 769-776.
12. Linley, E.; Denyer, S. P.; McDonnell, G.; Simons, C.; Maillard, J. Y. Use of hydrogen peroxide as a biocide: new consideration of its mechanisms of biocidal action. *J. Antimicrob. Chemother.* **2012**, *67*, 1589-1596.
13. Sunil, K.; Narayana, B. Spectrophotometric determination of hydrogen peroxide in water and cream samples. *Bull. Environ. Contam. Toxicol.* **2008**, *81*, 422-426.
14. Pupo Nogueira, R. F.; Oliveira, M. C.; Paterlini, W. C. Simple and fast spectrophotometric determination of $H_2O_2$ in photo-Fenton reactions using metavanadate. *Talanta* **2005**, *66*, 86-91.
15. Ribeiro, J. P. N.; Segundo, M. A.; Reis, S.; Lima, J. L. F. C. Spectrophotometric FIA methods for determination of hydrogen peroxide: Application to evaluation of scavenging capacity. *Talanta* **2009**, *79*, 1169-1176.
16. Klassen, N. V.; Marchington, D.; McGowan, H. C. E. $H_2O_2$ determination by the $I_3$-method and by $KMnO_4$ titration. *Anal. Chem.* **1994**, *66*, 2921-2925.
17. Rubio-Clemente, A.; Chica, E.; Peñuela, G. A. Rapid determination of anthracene and benzo(a) pyrene by high-performance liquid chromatography with fluorescence detection. *Anal. Lett.* **2017**, *50*, 1229-1247.
18. Pignatello, J. J.; Oliveros, E.; MacKay, A. Advanced oxidation processes for organic contaminant destruction based on the Fenton reaction and related chemistry. *Critical Rev. Environ. Sci. Technol.* **2006**, *36*, 1-84.
19. Sanches, S.; Leitão, C.; Penetra, A.; Cardoso, V. V.; Ferreira, E.; Benoliel, M. J.; Crespo, M. T.; Pereira, V. J. Direct photolysis of polycyclic aromatic hydrocarbons in drinking water sources. *J. Hazard. Mater.* **2011**, *192*, 1458-1465.